Supplementary Information

Multifunctional Phase Change Composites Enabled by Structurally Engineered Carbon Microtubule Aerogels for Efficient Thermal Energy Conversion and Storage

Shaokun Song,[a] Runze Wang,[a] Linda Lv,[a] Rui Feng,[a] Gangfeng Tan,[b]* Lijie Dong,[a] *

[a] Center for Smart Materials and Devices, State Key Laboratory of Advanced Technology for Materials Synthesis and Processing, School of Materials Science and Engineering, Wuhan University of Technology, Wuhan 430070, PR China

[b] School of Automotive Engineering, Wuhan University of Technology, Wuhan 430070, PR China

* Correspondence: auto_nova@whut.edu.cn (G Tan); dong@whut.edu.cn (L Dong)

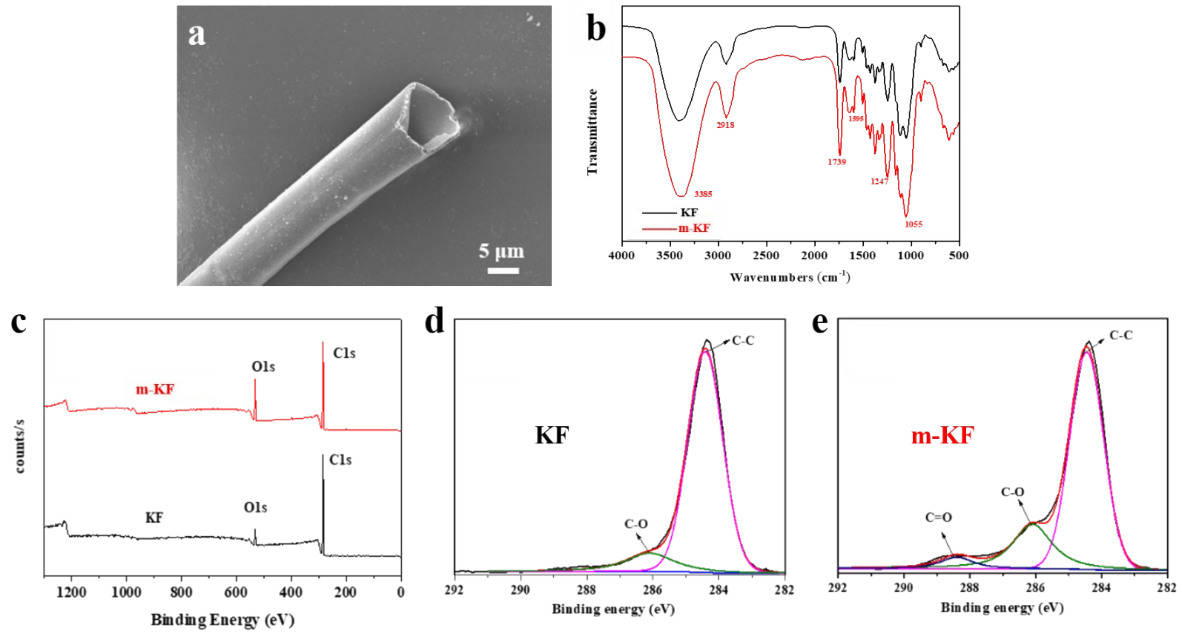

Figure S1. (a) Typical SEM image of KF; (b) FTIR and (c-e) XPS spectra of KF and m-KF.

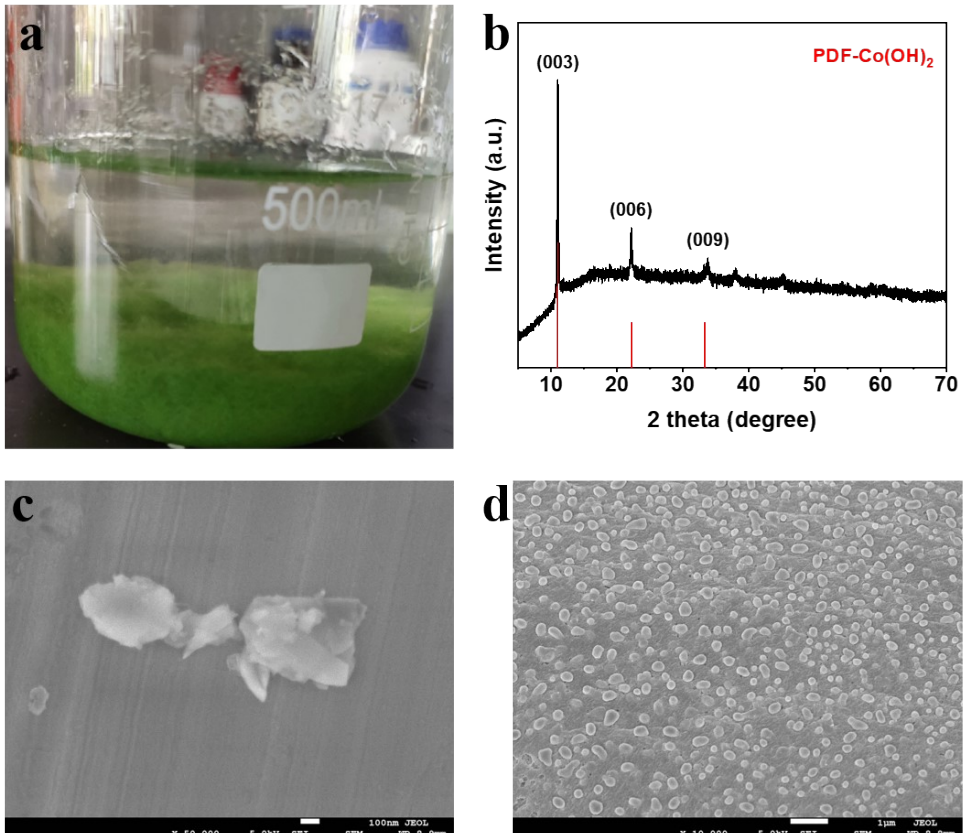

Figure S2. (a) Photograph of m-KF@$Co(OH)_2$; (b) XRD pattern and (c) SEM image of $Co(OH)_2$; (d) Local enlarged SEM images of CKF@CoNS.

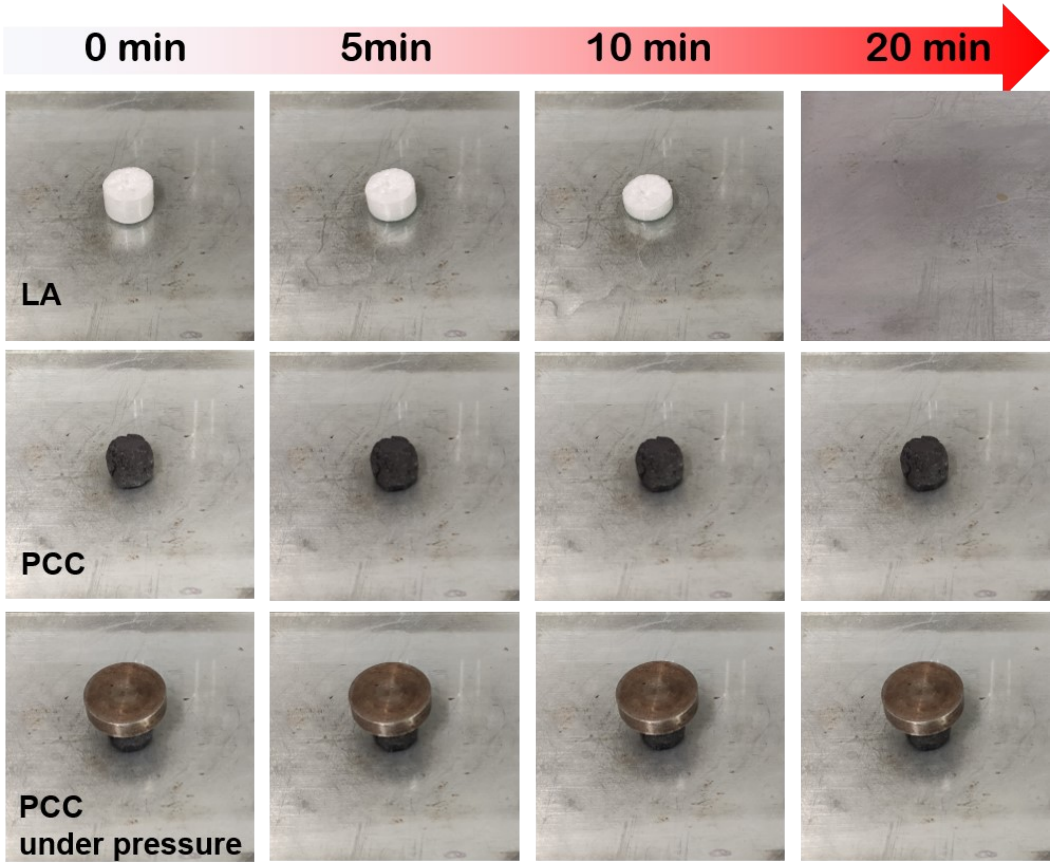

Figure S3. Shape-stability of LA and LA/CKF@CoNS-3.

Table S1. Thermophysical properties of LA/CKF@CoNS-5 after different thermal cycles.

Samples	Heating process		Cooling process		$\eta_{\Delta H}$ (%)
	T_m (℃)	ΔH_m (J/g)	T_c (℃)	ΔH_c (J/g)	
LA	43.3	194.1	39.6	197.2	100
0 cycles	42.8	179.9	41.4	186.2	92.7
100 cycles	43.0	180.4	40.3	187.7	92.9
500 cycles	42.5	181.0	41.2	187.0	93.3
1000 cycles	42.1	181.8	40.4	187.9	93.6
2000 cycles	43.1	181.5	41.5	188.4	93.5

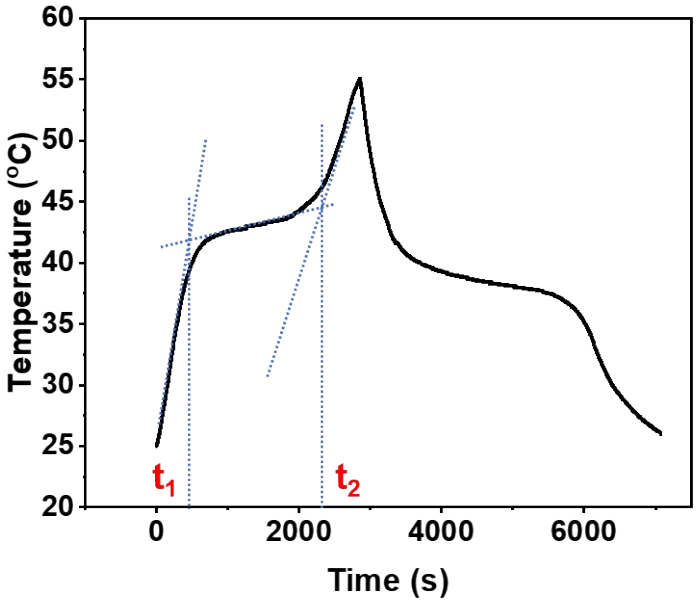

Figure S4. The method for determining the starting and terminating time points of samples.

Table S2. Photothermal conversion details of PCCs under different sun irradiation.

Sample	LA/CKF @1000 W/m²	LA/CKF@CoNS-5 @1000 W/m²	LA/CKF@CoNS-3 @1000 W/m²	LA/CKF@CoNS-1 @1000 W/m²	LA/CKF@CoNS-3 @700 W/m²	LA/CKF@CoNS-3 @1300W/m²
m (g)	1.1987	1.1987	1.1987	1.1987	1.1956	1.1956
S (cm^2)	4.4636	4.4636	4.4636	4.4636	4.4636	3.4636
ΔH (J/g)	184.1	179.9	181.5	182.8	181.5	181.5
P(W/m^2)	1000	1000	1000	1000	700	1300
t_1 (s)	285	263	169	263	323	186
t_2 (s)	1195	844	679	774	1249	656
t_2-t_1 (s)	910	581	510	511	926	470
η (%)	54.3	82.2	92.3	91.9	72.3	95.6